Applied Energy 419 (2026) 128139

Contents lists available at ScienceDirect

Applied Energy

journal homepage: www.elsevier.com/locate/apenergy

Spatially explicit planning of a sector-coupled energy system with hydrogen-related heat recovery for district heating

Longquan Li [a,*], Francesco Lombardi [b], Machteld van den Broek [b]

[a] Energy and Sustainability Research Institute Groningen, University of Groningen, the Netherlands
[b] Faculty Technology, Policy, and Management, Delft University of Technology, the Netherlands

HIGHLIGHTS

- A sector-coupled and spatially explicit model for Dutch energy system in 2050 is built.
- P2X and fuel cell heat recovery for district heating is modeled endogenously.
- Heat recovery cuts annualized system cost by 1.2 B€/yr.
- Heat recovery reduces DH heat pumps and battery capacity.
- Electrolyzer siting shifts toward provinces with stronger DH sinks.

ARTICLE INFO

Keywords:
Sector-coupling
Waste heat recovery
Hydrogen
District heating

ABSTRACT

Recoverable heat from electrolysis, fuel cells, and downstream hydrogen-to-X processes may provide an additional link between energy sectors. However, its system-level role and spatial implications remain insufficiently understood, as previous studies mainly focused on plant-level techno-economic assessments of individual technologies or local district-heating integration. This study addresses this gap using a spatially explicit optimization model of the Netherlands in 2050 to assess how hydrogen-related heat recovery affects the cost-optimal design of a sector-coupled energy system. The model optimizes both capacity and operation of supply, conversion, storage, and transmission technologies across Dutch provinces. Under base case assumptions, the results show that heat recovery reduces total annualized system cost by 2% (1.2 B€/yr), reduces battery capacity from 152 to 130 GWh and heat-pump capacity from 17 to 9 GW, while increasing electrolyzer capacity from 41 to 45 GW and underground hydrogen storage capacity from 33 to 37 TWh. Heat recovery substitutes part of dedicated district-heating supply and increases the use of hydrogen-related heat and hydrogen storage. Spatially, electrolyzer capacity shifts partly from locations mainly favored by renewable availability toward locations where recovered heat can be used in district heating, leading to greater use of hydrogen transmission infrastructure. Sensitivity analysis shows that higher district-heating shares moderately increase the value of heat recovery, while heat transport distance and hydrogen-cavern availability affect the strength of this effect. These findings show that hydrogen-related heat recovery can influence not only local heat utilization, but also technology competition, spatial siting, and infrastructure needs in sector-coupled energy-system planning.

Abbreviations: BTX, Benzene, Toluene, and Xylenes; CC, Carbon Capture; CO_2, Carbon Dioxide; DAC, Direct Air Capture; DEA, Danish Energy Agency; DH, District Heating; ETM, Energy Transition Model; H_2, Hydrogen; H_2-CHP, Hydrogen-based Combined Heat and Power; H_2-to-Methane, Hydrogen-to-Methane; H_2-to-Methanol, Hydrogen-to-Methanol; HP, Heat Pump; HT, High-Temperature; HVC, High-Value Chemicals; LT, Low-Temperature; MT, Medium-Temperature; OPSD, Open Power System Data; P2HH, Power-to-Hydrogen-and-Heat; P2X, Power-to-X; PEMEC, Proton Exchange Membrane Electrolyzer Cell; PEMFC, Proton Exchange Membrane Fuel Cell; PV, Photovoltaics; TES, Thermal Energy Storage.

* Corresponding author at: Energy Academy Europe Building, Nijenborgh 6, 9747 AG, Groningen, the Netherlands.
E-mail address: longquan.li@rug.nl (L. Li).

https://doi.org/10.1016/j.apenergy.2026.128139
Received 26 March 2026; Received in revised form 12 May 2026; Accepted 27 May 2026
Available online 31 May 2026

1. Introduction

Deep CO_2 emission reduction of future energy systems requires coordinated investment across electricity generation, electricity transmission, heat supply, and molecular energy carriers [1]. Sector coupling expands the feasible set of net-zero pathways by enabling electricity to be converted into heat and hydrogen, and by combining hydrogen and CO_2 to synthetic fuels, thereby creating cross-sector flexibility that can reduce curtailment and substitute for generation overbuild [2,3]. The main building blocks of sector coupling, as identified in the literature, are power-to-heat, power-to-hydrogen and power to synthetic fuel technologies, electrical and thermal storage, and the associated infrastructures such as district heating networks, electricity grids, and gas or hydrogen transport systems. Heat pumps and thermal energy storage are widely recognized as key enabling technologies for linking renewable electricity with heating demand, particularly where district heating systems are available [4–6]. Power-to-hydrogen becomes more relevant where direct electrification is constrained, where longer-duration balancing is required, or where molecular feedstocks remain necessary in industry and transport [7,8].

Within the sector-coupling context, recoverable heat from electrolysis, fuel cells, and downstream hydrogen-based conversion processes may provide an additional link between the power, hydrogen, fuel, and heating sectors. However, its system-level role remains insufficiently understood. Previous studies have shown that hydrogen- and P2X-related waste heat can improve efficiency and reduce costs under specific conditions. Existing work has mainly focused on plant-level techno-economic assessments, local district-heating (DH) integration, or specific case studies of electrolyzers and P2X facilities [9–15]. These studies indicate that the value of waste heat depends on factors such as heat transport distance, temperature matching, and the availability of heat pumps and thermal storage. However, they typically evaluate individual technologies or local heating systems in isolation. As a result, they do not capture how waste-heat utilization interacts with the broader supply-demand balance of multiple energy sectors, nor how it affects technology competition in a system with temporally resolved electricity, heat, hydrogen, and fuel demands.

Three key gaps therefore remain. First, although previous studies show that waste heat can be valuable locally, its effect on the cost-optimal technology portfolio of a multi-sector-coupled energy system is still unclear. It remains unknown how heat recovery changes the optimal mix of heat supply, storage, hydrogen conversion, and electricity-side flexibility options when multiple sectors are represented simultaneously and operated with temporally resolved supply and demand. Second, the spatial implications of waste-heat utilization remain poorly understood. Existing studies usually assess electrolyzers, fuel cells, or hydrogen-to-X processes in a predefined location, while the possibility that heat recovery itself may influence the preferred siting of these facilities has received little attention. Yet the value of recovered heat depends strongly on the spatial relationship between conversion facilities, DH demand, and interregional infrastructure. Third, previous studies suggest that heat transport distance affects the techno-economic feasibility of waste-heat use, while DH deployment affects the extent to which recovered heat can be absorbed. However, how these two factors shape the system value of heat recovery in a multi-sector-coupled energy system remains unknown.

This study addresses these gaps using a spatially explicit optimization model of the Netherlands in 2050. The analysis is guided by three questions. First, how does utilization of recoverable heat from electrolysis and selected hydrogen and P2X conversion processes affect the cost-optimal mix of technologies in a sector-coupled energy system? Second, how does waste-heat utilization affect the spatial distribution of key conversion technologies and the associated use of interprovincial infrastructure? Third, how do DH penetration and heat transport distance influence the value of recovered heat at the whole-system level?

This study makes three main contributions. First, it quantifies, in a temporally resolved multi-sector-coupled framework, how hydrogen- and P2X-related heat recovery changes the optimal technology portfolio across the electricity, heating, hydrogen, and synthetic-fuel parts of the system. Second, it shows how waste-heat utilization affects the spatial allocation of conversion capacity, particularly electrolyzer siting, and the resulting need for electricity and hydrogen transport infrastructure. Third, it evaluates how the system value of recovered heat varies under different assumptions on DH share, heat-recovery distance, and hydrogen-cavern availability, thereby identifying the conditions under which heat recovery becomes most valuable.

2. Methods

The modeling framework is implemented in Calliope (v0.7.7) [16] as a linear programming optimization problem that minimizes total annualized system cost subject to energy and material balance constraints, technology operation limits, and exogenous resource bounds. The system is represented as a multi-node, multi-carrier network in which each node corresponds to a Dutch NUTS2 region (NL11–NL42), hereafter referred to as provinces. The model target year is 2050, and the technology parameters have a projected value for 2050. Weather data from 2019 are used to represent renewable generation and demand conditions, including solar and wind capacity factors and demand profiles.

Hourly input profiles (solar and wind capacity factor and end-use demands) are resampled to 3-h timesteps for optimization. The 3-h resolution was selected to balance temporal detail and computational tractability. Because the model is spatially explicit and sector-coupled, hourly resolution would substantially increase the number of variables and constraints. A continuous full-year 3-h time series still captures daily and seasonal variations in renewable generation, demand, and storage operation. Previous work on multi-sector energy-system optimization also shows that coarser-than-hourly temporal resolution can greatly reduce computation time while causing only small differences in key outputs such as system cost and energy mix [17].

The optimization is solved using Gurobi. The objective is to minimize total annualized system cost, consisting of: (i) annualized investment costs, (ii) fixed operation and maintenance (O&M) costs, and (iii) variable operating costs proportional to energy (or material) throughput. All investments are annualized using a discount rate of 7.3%.

The model includes electricity, hydrogen (H_2), methanol, multiple heat carriers (individual heat, district heating, and industrial heat at low-, medium-, and high-temperature levels), and CO_2. International maritime and aviation fuels are not considered in this study.

Technologies are organized into five classes: (i) supply technologies that convert external resources into energy carriers, (ii) conversion technologies that convert carrier(s) to other carrier(s), (iii) storage technologies that shift carriers in time, (iv) transmission technologies that move carriers between nodes, and (v) demand technologies that represent final consumption or removal sinks (including curtailment and waste heat removal).

In the following sections, we provide further details on data sources and quantitative values utilized.

2.1. Energy demand representation

This section describes how end-use demands are represented in the provincial Netherlands model. We impose exogenous demands for electricity, hydrogen, individual heat, district heating, industrial process heat at three temperature levels, methanol, and CO_2. Electricity, heating and CO_2 demands are represented with 3-h profiles, while methanol demand is enforced as annual sink constraints. Table 1 reports the resulting annual demand totals by province and the data sources.

2.1.1. Electricity

Electricity demand includes electricity demands of residential and

Table 1
Annual demand totals by province [18,19].

	Electricity (TWh)	Hydrogen (TWh)	Individual heat (TWh)	District heat (TWh)	Industrial LT heat (TWh)	Industrial MT heat (TWh)	Industrial HT heat (TWh)	Methanol (TWh)	CO_2 (t)[a]
NL11 (Groningen)	5.4	0.0	2.5	1.6	1.7	0.5	0.0	6.4	0.0
NL12 (Friesland)	5.9	0.0	2.3	1.5	0.9	0.4	0.0	0.2	0.0
NL13 (Drenthe)	5.3	0.0	1.7	1.1	0.9	0.3	0.0	0.8	0.0
NL21 (Overijssel)	7.7	0.0	3.7	2.5	0.6	1.1	0.0	3.6	0.0
NL22 (Gelderland)	22.9	0.0	6.4	4.3	3.3	3.3	0.0	0.9	0.0
NL23 (Flevoland)	4.5	0.0	1.4	1.0	0.3	0.2	0.0	0.1	0.0
NL31 (Utrecht)	11.8	0.0	3.4	2.2	0.4	1.2	0.0	0.4	0.0
NL32 (North Holland)	30.2	5.1	9.9	6.6	1.9	0.8	2.5	0.0	937
NL33 (South Holland)	32.2	0.0	13.0	8.7	2.6	1.2	0.0	33.5	99
NL34 (Zeeland)	7.5	10.6	1.3	0.9	1.3	0.2	0.0	41.3	445,008
NL41 (North Brabant)	28.5	0.0	8.3	5.6	2.8	4.3	0.0	34.4	0.0
NL42 (Limburg)	13.7	0.0	3.9	2.6	1.4	3.4	0.0	41.4	1568
Total	175.6	15.7	57.8	38.6	17.9	17.0	2.5	163	447,612

[a] The CO_2 demand here represents the one in the fertilizer industry.

commercial building environment, agriculture, transport and the whole industrial subsectors. Annual electricity demand for households, buildings, agriculture, aluminum, other metals, food, paper and general industries is obtained directly from the Energy Transition Model (ETM) [20], a widely used source in the Netherlands, including for national reference scenarios made by all system operators [21]. The steel industry's electricity demand is computed as the product of provincial annual steel production and the specific electricity requirement of 820 kWh per t of steel, consistent with the H_2-DRI–EAF route used in sector-coupled Euro-Calliope [18]. For the fertilizer industry, electricity and CO_2 demand are derived from national ammonia and urea production volumes (1.8 Mt. and 1.3 Mt), using the assumptions that producing 1 t urea requires 0.92 MWh heat and 0.32 t CO_2, while producing 1 t NH_3 requires 0.178 t H_2 and 1.73 MWh electricity; the heat requirement is included in industrial process heat which is introduced below. These national totals are allocated to provinces based on current electricity consumption in the fertilizer sector reported in ETM. Road and rail transport are assumed to be fully electrified by 2050. Their electricity demand is estimated via dividing the fossil-fuel-based transport demand from ETM by a factor of 1.88, reflecting higher efficiency under electrification and the value 1.88 comes from the sector-coupled Euro-Calliope transport assumptions.

Hourly electricity demand curve for road transportation is taken from the sector-coupled Euro-Calliope dataset and the same curve is applied to all provinces. Electricity demand for steelmaking, fertilizer, and rail transportation is assumed to be constant over time. The demand curve for other electricity demands is taken from the OPSD (Open Power System Data) [22].

2.1.2. Individual and district heating

Total heat demand by province is obtained from ETM. Heat that is already electrified is excluded to avoid double counting. In the baseline scenario, 40% of provincial heat demand is assumed to be met through district heating and the remaining 60% through individual heating systems. Both heating categories use the same hourly demand profile derived from sector-coupled Euro-Calliope and are scaled to match annual totals.

The district-heating system considered in this study represents future low-temperature fourth-generation district heating rather than conventional high-temperature district heating. Fourth-generation district heating is designed to integrate low-temperature renewable and excess heat sources, with typical supply temperatures below those of conventional systems, often in the range of about 40–70 °C [5,23]. PEM electrolyzers commonly operate at approximately 50–80 °C, making their recoverable heat suitable for low-temperature district-heating integration, with heat pumps used for temperature upgrading when needed [24].

2.1.3. Hydrogen

Hydrogen demand is explicitly modeled for the steel and fertilizer industries. Annual hydrogen consumption is calculated from provincial production volumes and the corresponding specific consumption rates (H_2-DRI–EAF for steel; NH_3 production for fertilizers). Hourly hydrogen demand is assumed constant. Additional hydrogen use arises endogenously through P2X conversion routes (notably H_2-to-methane and H_2-to-methanol) and hydrogen-based electricity storage.

2.1.4. Industrial process heat

Industrial heat is divided into three temperature ranges following Rehfeldt et al. (2018): below 200 °C (LT), 200–500 °C (MT), and above 500 °C (HT). The steel sector is assigned to HT demand, food and paper industries to LT demand, and remaining sectors to MT demand. Annual heat demand for each temperature category is obtained from ETM. Hourly industrial heat demand is assumed constant throughout the year. It should be noted that the total annual demand of industrial heating (37.4 TWh) is significantly lower than the current value of >100 TWh, since we excluded the heating demand from the refinery and chemical sectors, which are major contributors to the current industrial heating demand.

2.1.5. Methanol

The methanol demand represents non-energy feedstock requirements linked to the chemical and plastics system boundary adopted in this study. In the sector-coupled Euro-Calliope framework, petrochemicals account for a large share of fossil feedstock use, and methanol is treated as a key low-carbon building block because high-value chemicals (HVCs) for plastics, e.g., ethylene/propylene/BTX(benzene, toluene, xylenes), can be produced via methanol-based routes (e.g., methanol-to-olefins/aromatics) instead of fossil naphtha/petroleum gas cracking [18]; methanol itself can be synthesized from CO_2 and H_2 or from biomass. Annual demand for methanol in the chemical sector is adopted from the sector-coupled Euro-Calliope assumptions and

allocated to provinces using non-energy feedstock demand in the chemical sector from the ETM dataset.

2.1.6. CO_2

CO_2 demand for the fertilizer industry is an exogenous input of the model, while CO_2 demand for methanol and methane production is endogenous when they are produced from the hydrogen-based routine.

2.1.7. Imports and curtailments

The Netherlands is and most probably will remain an energy importer for several reasons such as a large energy-intensive industrial sector. Possible energy import can be realized via different energy carriers, e.g., electricity, H_2, methanol, liquid organic hydrogen carriers [25]. We assume that methanol can be imported from other countries. Since we assume that methanol can only be produced from H_2 and CO_2 or biomass, the production of methanol is highly energy intensive. The Netherlands is a net exporter in the plastic industry, consuming 4.3% of converter plastics but produces 18% of EU-28's ethylene and propylene [18], which makes it a fair assumption for the Netherlands to import methanol from other countries.

Where required to maintain feasibility, surplus production can be curtailed or disposed of via dedicated 'removal' options (i.e., electricity curtailment and waste heat removal), which carry no service value but prevent artificial accumulation of energy carriers.

2.2. Supply technologies

The supply technologies include onshore wind, offshore wind, rooftop PV (Photovoltaics), utility-scale (open field) PV, biomass supply, and methanol import. Solar and offshore wind potentials are taken from the technical-social potential data by [26], with the redistribution of offshore wind potential to the provinces. The 70 GW potential from [26] is distributed to the provinces of Groningen (10 GW), North Holland (30 GW), South Holland (20 GW), and Zeeland (10 GW). These provinces have been planned by the Dutch government to have the most offshore wind connection [27]. Tröndle, Pfenninger and Lilliestam [26] also provided the technical-social potential for onshore wind of the Netherlands, which is 4.3 GW by 2050. However, the installed capacity in 2024 (7 GW) already exceeded this number. We assume the onshore wind potential of the Netherlands to be 15 GW by 2050, which is the same as [28], while the share in the provinces is identical to that in [26]. Capacity factors for solar and wind are taken from [29,30].

Biomass availability is represented through an upper bound on annual usable biomass energy. No minimum generation levels or intra-annual supply constraints are imposed; biomass conversion can therefore be scheduled freely within the year, subject only to the annual availability limit.

Regarding methanol imports, Sollai, Porcu [31] reported a levelized cost of renewable methanol production from green electrolysis hydrogen and carbon capture of 175 €/MWh. Transport costs of methanol import are ignored, and methanol imports are constrained only by their variable cost.

Table 2 shows the techno-economic parameters of the supply technologies, while Table 3 shows the potential of the generation technologies by province, with data sources specified via footnotes.

2.3. Storage and transmission technologies

Temporal flexibility can be provided by batteries, thermal energy storage (TES) for individual and district heating, and compressed hydrogen storage (tanks and salt caverns). Storage technologies are characterized by charge/discharge efficiencies, standing losses (where applicable), the ratio between power capacity and energy capacity, and investment and operating costs. Cavern-based underground hydrogen storage potential is concentrated in Groningen, Friesland, and Drenthe, with the capacity of 31, 4.2, and 8.1 TWh, respectively, according to [35].

Spatial coupling is represented by transmission links among provinces for electricity and hydrogen transport. Electricity transmission is modeled as brownfield, existing capacity of the electricity grid does not add any investment to the system. The existing high-voltage transmission capacity between provinces is generated by making use of the PyPSA-Eur workflow [36], and the resulting transmission capacity is shown in Table 4. It's assumed that there is no cross-border import and export of electricity with neighboring countries. Tables 5 and 6 show the techno-economic parameters of storage and transmission technologies, respectively.

2.4. Conversion technologies

In this study, different conversion technologies are modeled. Fig. 1 and Table 7 show the energy and mass flows, and parameters of these technologies. For Power-to-Heat technologies, electric heaters and heat pumps (HP) at different scales can be used to supply either individual heat or district heating, high-temperature HP (up to 150 °C) for industrial LT heating demand, and direct electric firing for MT and HT industrial heating demands. Methane boilers and biomass boilers are modeled for residential heat, district heating, or LT industrial heating, and biomass firing, and methane firing for MT and HT industrial heating demands. For hydrogen-related conversion, the model includes P2HH based on electrolysis, hydrogen-based fuel cell for combined heating and power generation (H_2-CHP), downstream P2X synthesis routes converting hydrogen and CO_2 into methane and methanol, and hydrogen boilers for LT industrial heating demand. CO_2 can be supplied by direct air capture (DAC) and by carbon capture (CC) from biomass boilers to provide CO_2 for synthetic fuel production.

Waste heat is represented as a heat carrier that can be delivered to district heating via dedicated heat transmission over a certain distance. We assume a heat transmission distance of 200 m for the heat recovery from electrolyzer and fuel cell to a connecting point from the DH system, which can be for instance the storage unit of the DH system. This distance is consistent with that from [9]. For heat recovery from P2X processes, we assume a longer transport distance of 5 km, consistent with empirical evidence on present-day spatial proximity between industrial excess heat sources and district heating areas [39]. The hydrogen-related waste heat can also be curtailed.

2.5. Scenario design and sensitivity cases

We run multiple scenarios. The ref. scenario represents the energy system introduced by section 2.1–2.4, while the rest of the scenarios

Table 2
Techno-economic parameters for generation technologies.

Technology	Output carrier	Lifetime (yr)	CAPEX ($€_{2020}$/kW)	Fixed O&M fraction (%/CAPEX)	Variable OPEX (($€_{2020}$/MWh))	Ref
Open field PV	Electricity	40	290	2.5	–	Utility-scale PV in [32]
Rooftop PV	Electricity	40	520	1.6	–	Rooftop PV residential in [32]
Onshore wind	Electricity	30	1090	1.4	1.8	Onshore turbines in [32]
Offshore wind	Electricity	30	1990	1.4	2.8	Offshore Wind AC Fixed in [32]
Biomass supply	Biomass	–	–	–	40[a]	[33]
Methanol import	Methanol	–	–	–	175	[31]

[a] This is the current cost for biomass feedstock supply.

Table 3
Renewable energy potential and existing nuclear capacity by province in Netherlands.

Node	Open field PV potential (GW)[a]	Rooftop PV potential (GW)	Onshore wind potential (GW)[a]	Offshore wind potential (GW)	Biomass availability (TWh)[b]
NL11 (Groningen)	2.4	5.2	1.2	10	3.7
NL12 (Friesland)	6.3	7.4	0.7	0.0	3.7
NL13 (Drenthe)	2.1	6.1	1.0	0.0	2.2
NL21 (Overijssel)	2.4	12.5	0.5	0.0	4.0
NL22 (Gelderland)	1.7	22.1	0.3	0.0	5.6
NL23 (Flevoland)	0.3	3.5	0.5	0.0	2.4
NL31 (Utrecht)	1.4	8.5	0.2	0.0	2.6
NL32 (North Holland)	1.2	16.0	0.7	30	5.7
NL33 (South Holland)	1.7	23.9	0.3	20	6.5
NL34 (Zeeland)	0.1	5.2	0.7	10	3.7
NL41 (North Brabant)	0.8	29.9	0.9	0.0	7.0
NL42 (Limburg)	0.3	14.1	0.3	0.0	3.1
Total	20.7	154.4	7.5	70	50.2

[a] The capacity for open field PV and onshore wind indicates a land use area of 2100 km^2 [26].
[b] Biomass availability of each province is taken from [19], and the sum of the biomass potential in all the provinces matches the actual amount of bioenergy used in Netherlands in 2022, according to [34].

Table 4
Existing electricity transmission capacity between the provinces in Netherlands.

Location	Capacity (GW)
NL11 to NL12	1.4
NL11 to NL13	0.7
NL11 to NL21	2.4
NL12 to NL23	0.7
NL13 to NL21	0.7
NL21 to NL22	2.4
NL21 to NL23	3.1
NL22 to NL41	2.4
NL23 to NL32	2.4
NL31 to NL32	2.4
NL31 to NL33	2.4
NL32 to NL33	2.4
NL33 to NL41	2.4
NL34 to NL41	2.4
NL41 to NL42	4.8

modifies certain subset of input, while keeping all other configurations of the model identical to the ref. scenario. The no_hr scenario is used to assess the role of heat recovery. The no_caverns and no_caverns_no_hr scenarios are introduced to evaluate the importance of underground hydrogen storage, with and without heat recovery. The heat_distance_short, heat_distance_long, and heat_distance_10 km scenarios test the sensitivity of the results to heat recovery distance. Finally, the dh0_3, dh0_5, and dh0_6 scenarios, together with their corresponding no_hr variants, are used to examine how the system responds to different district heating shares. Table 8 provides an overview of all scenario runs and their key assumptions.

3. Results

This section first presents the main results from the ref. and no_hr scenarios (Section 3.1 and 3.2), before assessing the robustness of the identified patterns across the sensitivity scenarios (Section 3.3). To keep the main text focused on the most relevant system-level changes, detailed results for all scenarios—including technology capacities, annual aggregated flows, and annualized costs—are reported in the Supplementary Material (A), and the model validation is presented in Supplementary Material (B).

3.1. System-level results (national aggregates)

At the system level, removing heat recovery increases the total annualized system cost by 2% (Table 9). Wind, solar, and biomass are all utilized up to their available limits in both scenarios, and methanol imports are needed. Methanol demand decreases by 4%, while electricity curtailment increases by 22% with heat recovery.

Table 6
Techno-economic parameters for transmission technologies [38].

Technology	Carrier	Lifetime (yr)	Efficiency [a]	CAPEX ($€_{2020}$/kW/km) [b]	Fixed O&M fraction (%/CAPEX)
Existing high-voltage cables	Electricity	60	0.98	0	0
High-voltage cables	Electricity	60	0.98	0.62	1.5
H2 pipeline	H_2	50	1	0.4	4

[a] transmission distance between the provinces is assumed to be 50 km to ease the efficiency calculation.
[b] The CAPEX data for both electricity and hydrogen transmission are based on a capacity of 2 GW.

Table 5
Techno-economic parameters for storage technologies [37].

Technology	Carrier	Lifetime (yr)	Power capacity per energy capacity	Round efficiency	Storage loss (%/h)	CAPEX ($€_{2020}$/kWh)	Fixed O&M fraction (%/CAPEX)	Variable OPEX (($€_{2020}$/MWh))
Battery	Electricity	20	1	0.91	0	280	2.9	0
Tank_H_2	H_2	30	0.005	0.90	0	22	2	0
Cavern_H_2	H_2	100	0.001	0.99	0	1.3	0.2	0
TES_individual	Heat	30	6.7	1	0.008	420	4	0.1
TES_DH	DH heat	40	0.02	0.98	0.008	3	0.3	0

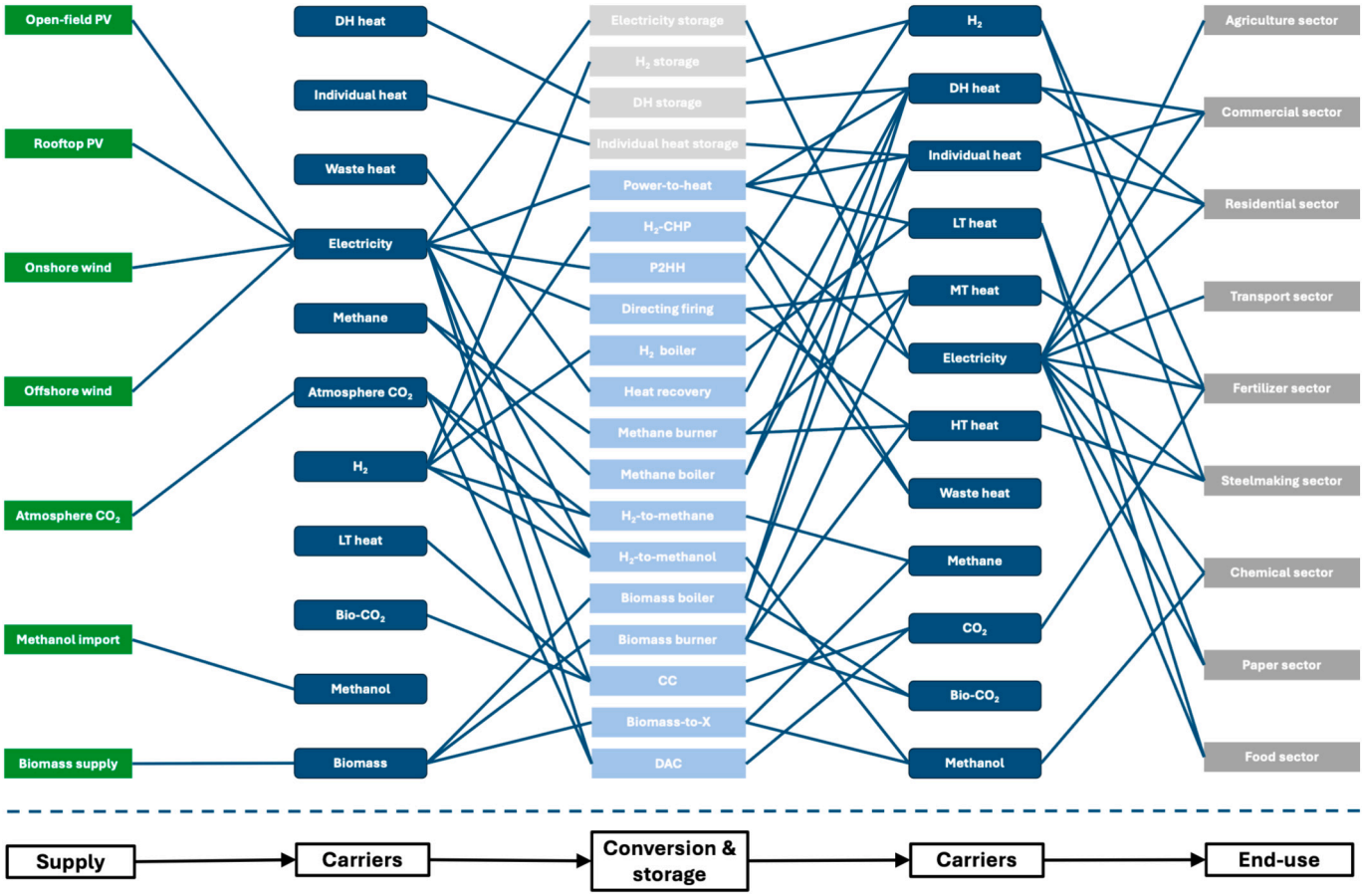

Fig. 1. The energy and mass flows of the sector-coupled energy system in this study.

The cost breakdown shows which technologies provide this compensation (Fig. 2). Horizontal bars show the change in total annual cost by technology, calculated as no_hr minus ref., for the top contributors and an aggregated "Other" category for all rest technologies. Positive values indicate higher cost in no_hr scenario and negative value indicate the opposite. The right columns report the reference-scenario capacity [Cap(ref)] and the capacity change [ΔCap = no_hr − ref]. For Methanol import, capacity is represented by annual energy flow (in GWh). For technologies with multiple inputs/outputs (Electrolyzer, Fuel cell, and H_2-to-Methanol), capacity is defined as the energy flow capacity of the output carrier with the highest capacity (in GW). For storage technologies, capacity is represented by energy storage capacity in GWh. All other technologies use energy flow capacity in GW. Without heat recovery, cost increases mainly due to more battery storage, methanol imports, and district heating heat pumps, while cost reduce due to less need for H_2 cavern storage, fuel cells, and electrolyzers.

Fig. 3 shows how heat recovery changes the DH supply mix over the year. Fig. 3 (a) shows the daily recovered-heat share in DH heat supply for REF and NO_HR. Recovered heat is defined as the combined DH heat delivered via Heat recovery (200 m and 5 km). Fig. 3 (b) shows the daily DH heat supply by source with daily DH heat demand overlaid (black line) in the ref. scenario. The stacked sources are Heat recovery (200 m), Heat recovery (5 km), DH TES (discharge), Heat pump (DH), and Other (all remaining minor DH supply sources). Fig. 3 (c) represents the same figure as in (b), but for no_hr scenario. Annual totals shown in the legends are obtained by summing the corresponding daily series over the full year. In the ref. scenario, recovered heat supplies a clear share of DH heat, while in no_hr scenario this share is zero. The daily supply decomposition indicates that recovered heat is mainly provided by Heat recovery (200 m), with Heat recovery (5 km) contributing a smaller additional part. As recovered heat increases, the contribution of the Heat pump (DH) decreases, showing that recovered heat substitutes part of electrified DH supply. In contrast, the annual contribution of DH TES (discharge) is similar in both cases, suggesting that heat recovery changes the composition of DH supply rather than increasing the annual discharge of thermal storage. Overall, the figure supports that the main effect of heat recovery in DH supply is a replacement of DH heat-pump output by recovered heat, dominated by the heat recovery from fuel cell and electrolyzers.

Heat recovery also affects the operation of key flexibility technologies (Fig. 4). Time series of storage levels and key system flows over the simulated year. Panels show (a–d) storage levels of batteries, hydrogen caverns, district heating thermal energy storage (DH TES), and individual TES; (flow_in); (e) methanol production from hydrogen; (f) methanol production from biomass; and (g) renewable curtailment. Blue solid lines represent the reference scenario and red dashed lines the no-HR scenario. The right column reports the corresponding annual flows in TWh (Outlet energy flow for all technologies except curtailment, which represents inlet energy flow). Battery output increases by 15%, indicating a larger role for short-term electricity balancing in the no_hr case. By contrast, H_2 cavern output decreases by 6% (ref: 54.9 TWh; no_hr: 51.6 TWh), consistent with the lower cavern investment shown in Fig. 2. H_2-to-methanol is an important flexibility asset in the system, as the methanol demand only needs to be satisfied throughout the year. Without heat recovery, domestic methanol production is decreased and instead more methanol is imported. H_2-to-methanol output and biomass-to-methanol decreases by 5% and 7%., respectively.

Thermal storage shows a varied response with respect to the annual total and the temporal pattern. For DH TES, annual output changes by about 1%, while the temporal pattern changes much more. The storage

Table 7
Techno-economic parameters for conversion technologies.

Technology	Input carrier(s)	Output carrier (s)	Lifetime (yr)	Efficiencies	CAPEX [a]	Fixed O&M fraction (%/CAPEX)	Variable OPEX (($€_{2020}$/MWh))	Ref
P2HH	Electricity	H_2, Waste heat (200 m)	25	0.8 (H_2), 0.17 (Heat)	326	2	–	PEMEC 1 GW in [40]
H_2-CHP	H_2	Electricity, Waste heat (200 m)	10	0.42 (electricity), 0.34 (heat)	850	5	–	LT-PEMFC CHP in [32]
Biomass-to-Methanol	Biomass	Methanol	20	0.65	1550	2.6	14.5	Methanol biomass gasif. In [40]
Biomass-to-methane	Biomass	Methane	20	0.7	1595	1.6	1.7	Gasif. CFB, Bio-SNG in [40]
H_2-to-Methanol [b]	H_2, CO_2, Electricity	Methanol, Waste heat (5 km)	30	See table note	870	2.9	–	Methanol from hydrogen in [40]
H_2-to-Methane [c]	H_2, CO_2	Methane, Waste heat (5 km)	20	See table note	318	5	–	[41]
Electric heater	Electricity	Individual heat	30	1	900	0.9	–	Electric heating, new single in [42]
Individual HP [d]	Electricity	Individual heat	20	See table note	1700	3.6	–	HP air-water, new single in [42]
Individual biomass boiler [e]	Biomass	Individual heat	20	0.85	550	8.5	0	Biomass auto, new single in [42]
Individual methane boiler	Methane	Individual heat	20	0.99	274	4.8	–	Gas boiler, new single in [42]
Electrode heater	Electricity	DH heat	25	0.99	60	1.6	1	Electric boiler, large in [32]
DH HP [d]	Electricity	DH heat	25	See table note	810	0.2	2.7	Comp. hp., air source 10 MW in [32]
DH biomass boiler [e]	Biomass	DH heat, Biogenic CO_2	25	1 (Heat)	430	7.8	2.5	Wood Chips HOP, large in [32]
DH methane boiler	Methane	DH heat	25	1	50	3.6	1.0	Natural Gas DH Only in [32]
LT industrial biomass boiler [e]	Biomass	LT industrial heat, Biogenic CO_2	15	1 (Heat)	740	4.8	1.5	Boiler, biomass in [43]
LT industrial H_2 boiler	H_2	LT industrial heat	20	0.94	42	3.7	0.9	[44]
LT industrial methane boiler	Methane	LT industrial heat	25	1	90	2.2	1.2	Boiler, gas and oil in [43]
Industrial HP	Electricity	LT industrial heat	20	3	1350	0.2	3.4	High temp. hp. Up to 150 in [43]
MT industrial direct firing burner [f]	Electricity	MT industrial heat	20	0.8	70	0	0.2	Direct electric firing in [43]
HT industrial direct firing burner [f]	Electricity	HT industrial heat	20	0.8	70	0	0.2	Direct electric firing in [43]
MT industrial biomass burner [f]	Biomass	MT industrial heat, Biogenic CO_2	15	0.8	260	1.4	0.17	Direct firing Solid Fuels in [43]
HT industrial biomass burner [f]	Biomass	HT industrial heat, Biogenic CO_2	15	0.8	260	1.4	0.17	Direct firing Solid Fuels in [43]
MT industrial methane burner [f]	Methane	MT industrial heat	15	0.8	18	1	0.11	Direct firing Natural Gas in [43]
HT industrial methane burner [f]	Methane	HT industrial heat	15	0.8	18	1	0.11	Direct firing Natural Gas in [43]

(*continued on next page*)

Table 7 (*continued*)

Technology	Input carrier(s)	Output carrier (s)	Lifetime (yr)	Efficiencies	CAPEX [a]	Fixed O&M fraction (%/CAPEX)	Variable OPEX (($€_{2020}$/MWh))	Ref
DAC [g]	Electricity	CO_2	30	0.0008	1600	3.8	5	Liquid Direct Air Capture in [45]
CC from biomass boiler [h]	Biogenic CO_2 Electricity LT industrial heat	CO_2	25	See table note	1900	3.1	–	Post comb – Large biomass in [45]
Heat recovery (200 m)	Waste heat (200 m)[i]	DH heat	45	0.9995	6	0.3	–	DH transmission in [38]
Heat recovery (5 km)	Waste heat (5 km)[j]	DH heat	45	0.99	155	0.3	–	DH transmission in [38]

[a] The CAPEX unit for electrolyzer and fuel cell is €2020/kWe, for heat pump, electric heaters, heat transmission, and boilers is $€_{2020}/kW_h$, for DAC and CC is $€_{2020}/kt_{CO2}/h$, for methane generators is $€_{2020}/kW_{methane}$, for methanol generators is $€_{2020}/kW_{methanol}$.

[b] The methanol and waste heat production efficiency based on H_2 and electricity inputs is 0.78 and 0.2, respectively. CO_2 demand is 1.4 $t/t_{methanol}$, the electricity demand is 0.1 $MWh/t_{methanol.}$ Steam demand is assumed to be satisfied by H_2.

[c] The methane and waste heat production efficiency based on H_2 input is 0.83 and 0.15, respectively. CO_2 demand is 0.2 $t/MWh_{methane.}$

[d] HP efficiency for individual and DH heating has a temporal profile.

[e] Efficiency of CO_2 generation from biomass boilers: 0.36 $t/MWh_{bio.}$

[f] The efficiency for industrial direct firing is taken as the system efficiency, instead of the efficiency of the burner itself, which can range from 0.5 to 0.95 depending on system types. We assume the value to be 80%.

[g] DAC efficiency unit: t_{CO2}/kWh_{el}, with the heating demand is assumed to be electrified.

[h] This technology is CO_2 capture from the flue gas of biomass boilers and burners. The CO_2 capture rate is 95%, electricity demand is 20 kWh/t_{CO2}. Heating demand in the capture has a temperature level of 130–150 °C, and is modeled as an endogenous LT industrial heating demand, and the value of this heat demand is 660 kWh/t_{CO2}.

[i] The heat from fuel cell and electrolyzer.

[j] the heat from H2-to-X.

Table 8
Scenario runs in this study.

Scenario label	Heat recovery	H2 caverns availability	Heat recovery distance from P2HH and H_2-CHP (km)	Heat recovery distance from H_2-to-X (km)	DH share to overall heat demand
ref	●	●	0.2	5	0.4
no_hr	○	●	–	–	0.4
no_caverns_no_hr	○	○	0.2	5	0.4
no_caverns	●	○	0.2	5	0.4
heat_distance_short	●	●	0.2	0.2	0.4
heat_distance_long	●	●	5	5	0.4
heat_distance_10 km	●	●	10	10	0.4
dh0_6-10 km	●	●	10	10	0.6
dh0_6	●	●	0.2	5	0.6
dh0_6-no_hr	○	●	–	–	0.6
dh0_5	●	●	0.2	5	0.5
dh0_5-no_hr	○	●	–	–	0.5
dh0_3	●	●	0.2	5	0.3
dh0_3-no_hr	○	●	–	–	0.3

●: yes.
○: no.

trajectory shows distinct operating styles: in the ref. scenario, the state-of-charge exhibits more sustained plateaus and clearer seasonal build-up and drawdown phases, whereas in the no_hr scenario the profile is more fragmented and characterized by intermittent peaks. This indicates that heat recovery mainly changes how DH TES is scheduled over the year, rather than increasing its annual utilization. Fig. 3 suggests that, in summer, Heat recovery (200 m) already covers a large share of DH demand in the ref. scenario, thereby reducing the need for TES discharge during these periods and leading to a smoother seasonal storage trajectory. The change in individual TES, by contrast, appears to be driven less by heat recovery directly than by changes in the individual heating technology mix. As shown in Fig. 2, the capacities of individual methane boilers and individual biomass boilers also differ between the two scenarios, and this reallocation of individual heat supply technologies changes the optimal magnitude of individual TES.

3.2. Spatial patterns and node-level results

Fig. 5 provides a province-level view of how technology capacities are reallocated under heat recovery. The upper panel presents absolute annual values in the ref. scenario, including electricity demand, DH demand, recovered heat, wind and PV generation, and methanol demand. The middle panel presents the absolute capacities of selected technologies in the ref. scenario. The lower panel shows the relative capacity change of these technologies to the no_hr scenario. Positive values indicate higher capacities in the reference case, whereas negative

Table 9
System-level key performance indicators in 2050 (national totals) for ref. (heat recovery allowed) and no_hr (heat recovery disallowed).

Parameter	Unit	ref	no_hr
Total annualized system cost	B€/yr	59.5	60.6
Electricity curtailment	TWh/yr	5.5	4.3
Methanol import	TWh/yr	91.9	95.5
Renewable generation – Wind onshore	TWh/yr	15.9	15.9
Renewable generation – Wind offshore	TWh/yr	182.6	182.6
Renewable generation – PV open-field	TWh/yr	22.5	22.5
Renewable generation – PV rooftop	TWh/yr	168.4	168.4
Renewable generation – total (wind+PV)	TWh/yr	389.3	389.3
Biomass supply (energy)	TWh/yr	50.2	50.2
Total end-use demands	TWh/yr	488.1	488.1

values indicate higher capacities in the no_hr scenario. Across provinces, the amount of recovered heat is positively correlated with DH demand: provinces with higher DH demand generally also exhibit higher heat recovery levels. In most provinces, the recovered heat is dominated by Heat recovery (200 m), which represents heat recovered from fuel cells and electrolyzers. By contrast, large-scale Heat recovery (5 km) appears only in a few provinces with high methanol demand, notably NL33, NL41, and NL42, where heat recovered from the H_2-to-methanol route becomes significant.

A clear pattern emerges for electrolyzer capacity. In most provinces, electrolyzer capacity increases under heat recovery, whereas it decreases only in a few provinces with exceptionally high wind and PV generation, such as NL11, NL32, and NL34. This indicates that heat recovery changes the preferred spatial allocation of electrolyzers. Without the additional value of recoverable heat, electrolyzers are more strongly attracted to locations with abundant renewable electricity. When heat recovery is enabled, however, electrolyzer deployment shifts toward provinces where the recovered heat can be utilized in district heating systems, suggesting that heat recovery becomes an additional siting driver alongside renewable resource availability.

Heat pump capacity decreases in all provinces, which indicates that recovered heat substitutes mostly the heating supply otherwise provided by heat pumps. The magnitude of this decline differs across provinces. In provinces where the substitution effect is strongest, reflected by the largest reductions in heat pump capacity, DH TES capacity tends to increase, as seen in NL11, NL32, and NL34. This suggests that when recovered heat plays a larger role in the heating mix, additional thermal storage is needed to balance temporal mismatches between heat supply and DH demand.

The flexibility mix also changes systematically. Battery capacity decreases in nearly all provinces, while fuel cell capacity, used here as an indicator of hydrogen-based electricity storage, increases in most provinces. This contrast suggests a shift in system flexibility away from battery-based electricity storage and toward the electricity-hydrogen-electricity cycle in a scenario with heat recovery. This can be explained

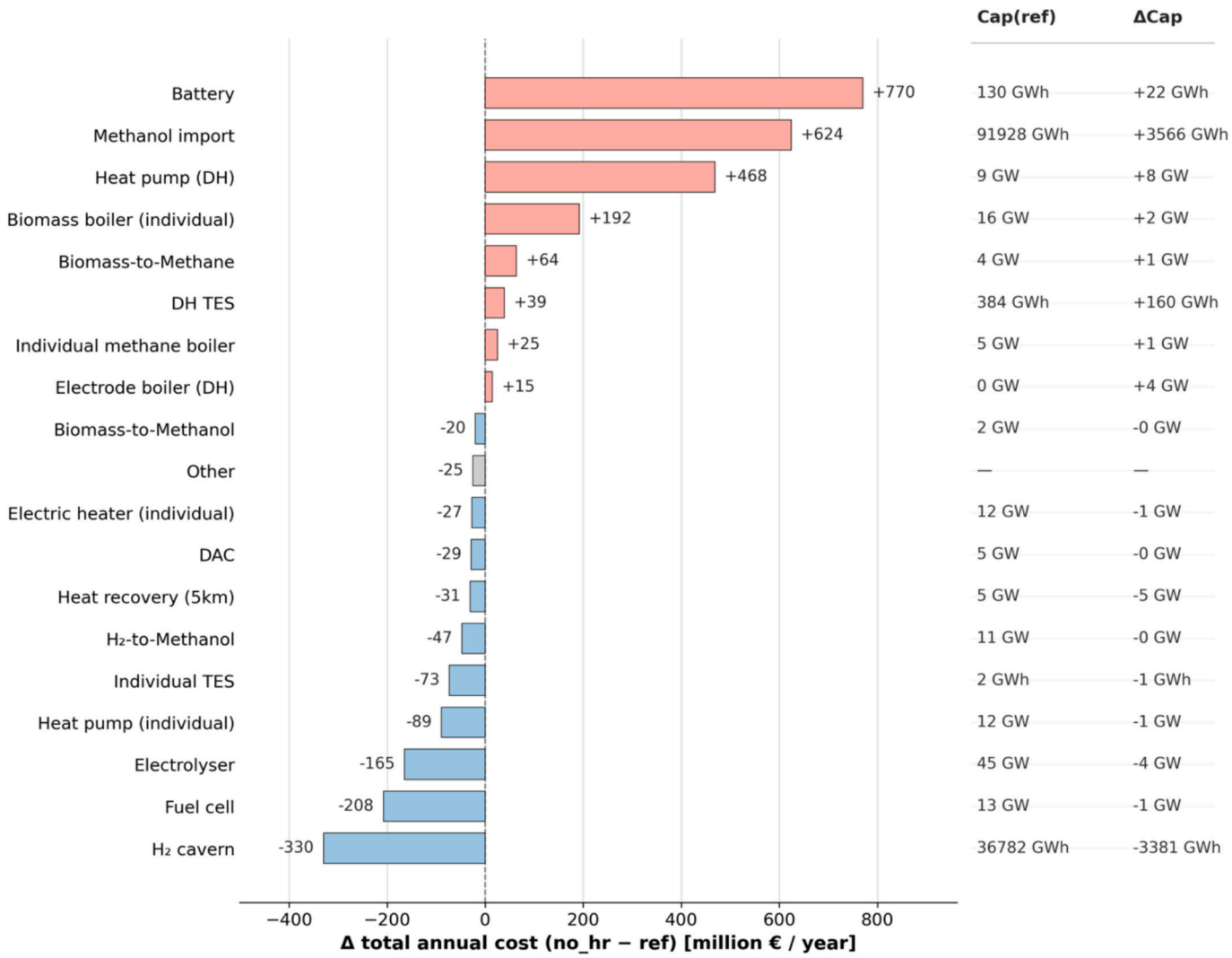

Fig. 2. Change in annual total system cost by technology between the no_hr and ref. scenarios, with capacities in the ref. scenario and capacity changes.

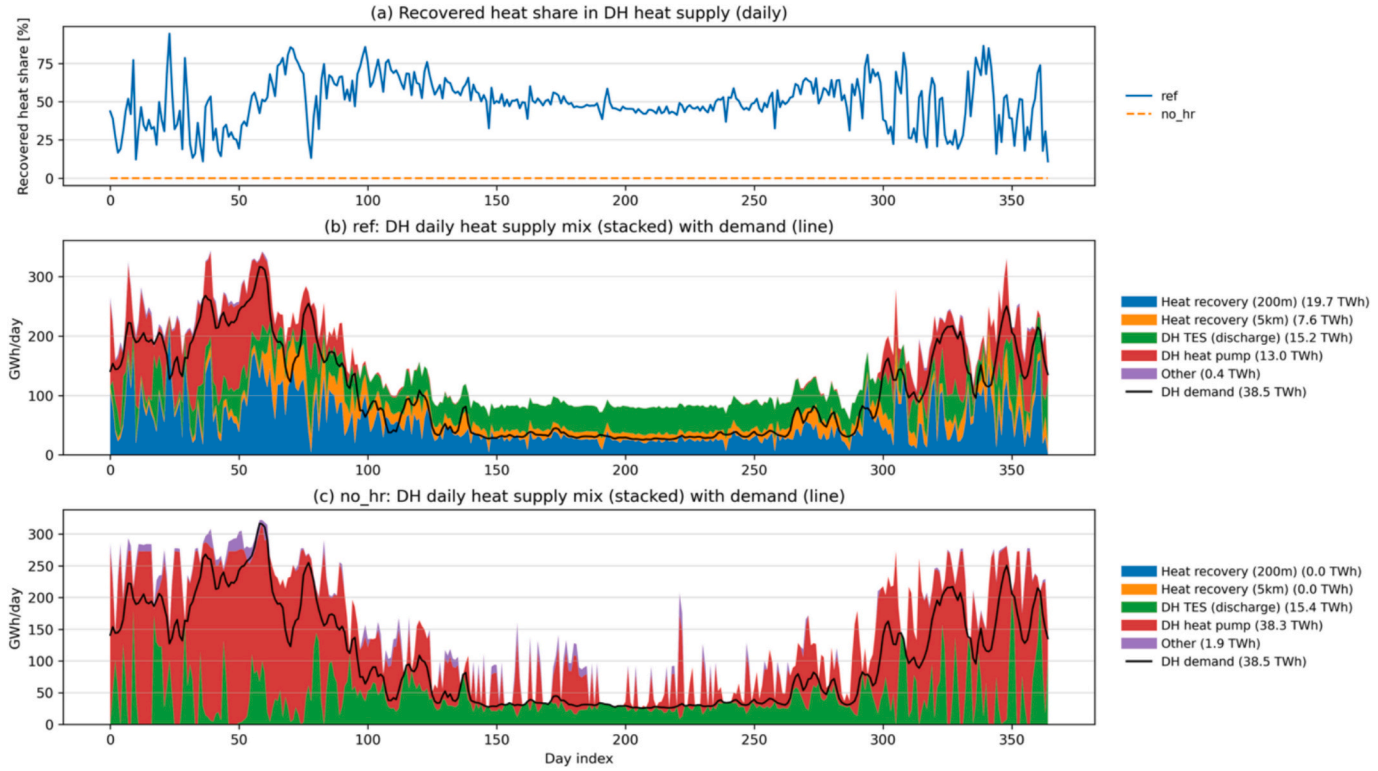

Fig. 3. Daily district-heating (DH) supply mix and recovered-heat share for the ref and no_hr scenarios.

by the fact that, when heat recovery is available, part of the energy otherwise lost during the hydrogen round-trip can be utilized as useful heat. As a result, the effective efficiency disadvantage of hydrogen-based electricity storage is partly mitigated at the system level, improving its relative attractiveness compared with batteries.

Fig. 6 summarizes how allowing heat recovery reshapes the expansion of interprovincial energy infrastructures. Red lines indicate higher expansion requirements in no_hr than in ref., while blue lines indicate higher expansion requirements in ref. Line width is proportional to the absolute capacity difference. The results show an opposite reallocation between electricity and hydrogen networks. In the no_hr case, several central and eastern corridors require more new electricity transmission capacity (Fig. 5a). In the ref. case, the system relies more strongly on new hydrogen pipeline capacity, especially across parts of the northern and central network (Fig. 5b). This can be linked to the electrolyzer siting pattern discussed above: with heat recovery, electrolyzer capacity becomes more spatially decentralized, while hydrogen demand remains concentrated in specific provinces. As a result, more hydrogen needs to be transported across provinces from dispersed production sites to concentrated demand locations, increasing the expansion requirement of the hydrogen network. At the same time, the need for long-distance electricity transmission is reduced.

3.3. Sensitivity analysis

To assess the robustness of the findings in Section 3.2, we evaluate additional sensitivity cases. The sensitivity analysis tests three sources of uncertainty that are directly linked to the model formulation: the district heating (DH) share in final heat demand, the assumed transport distance for recovered heat, and the availability of H_2 cavern storage. Table 10 summarizes key system-level indicators for all scenarios and is used for the comparisons below. Sys. cost is the total annualized system cost. HR benefit is defined as the reduction in system cost relative to the paired no-heat-recovery scenario. HR used is the annual amount of recovered heat utilized. DH HP refers to installed district heating heat pump capacity. Elec. trans. and H_2 pipe report the total newly built electricity transmission and hydrogen pipeline capacities.

3.3.1. Impact of district heating share

The cost advantage of heat recovery remains positive across all tested DH-share cases. In the paired comparisons, the system-cost reduction remains around 1.2 B€/yr. This indicates that the cost-effectiveness of heat recovery is robust over the tested range. In every paired comparison, heat recovery substantially reduces DH heat-pump capacity. At the same time, heat recovery consistently lowers battery capacity, increases electrolyzer capacity, reduces electricity-transmission expansion, and increases hydrogen-pipeline expansion.

The response of recovered heat utilization to DH share is not strictly linear, and the dh0_3 scenario already shows slightly higher recovered-heat utilization than the ref. scenario. This suggests that expanding district heating enlarges the available sink for recovered heat, but the extent of utilization is also shaped by system-wide interactions rather than by DH share alone.

3.3.2. Impact of heat recovery distance

Increasing the heat recovery distance leads to a slight increase in total system cost and a slight reduction in recovered heat utilization. It is also associated with modest decreases in battery capacity and modest increases in H_2 cavern capacity. The dh0_6-10 km scenario, with a 60% DH share and a 10 km heat-recovery distance, confirms that heat-recovery distance has only a minor effect under higher DH penetration. Recovered heat use remains 31 TWh/yr, almost unchanged from 32 TWh/yr in dh0_6. This suggests that, when sufficient DH demand is available, recovered heat utilization is mainly constrained by available heat demand rather than by the heat-recovery distance within the tested range.

3.3.3. Impact of H_2 cavern availability

Removing H_2 cavern availability leads to a stronger change in system structure than the distance sensitivity. When caverns are unavailable,

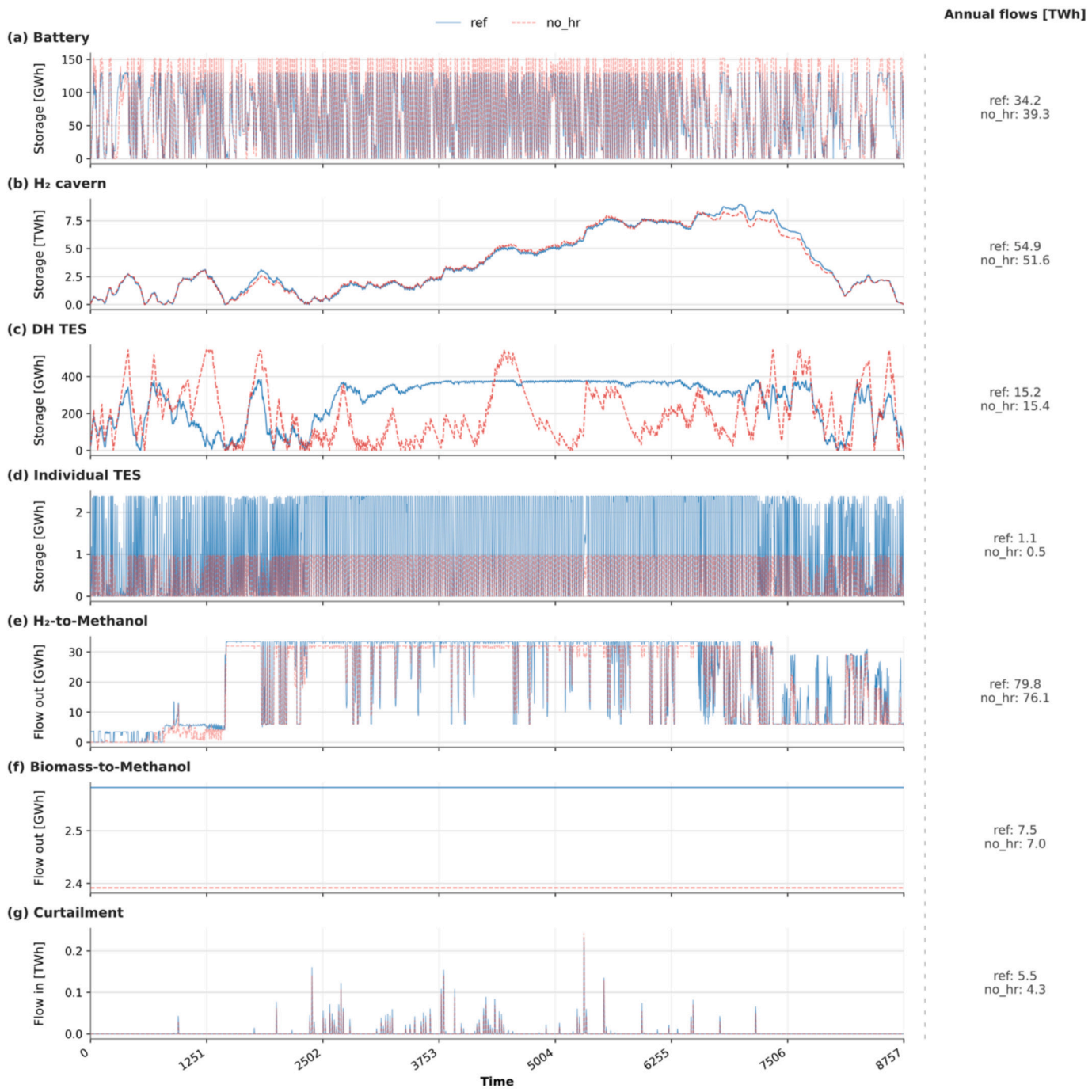

Fig. 4. Storage dynamics and operation of other flexibility sources under the reference and no-hr scenarios.

total annualized system cost increases substantially relative to the reference pair. The system shifts toward electricity-side investments, as indicated by much higher battery capacity, while electrolyzer capacity decreases. This confirms that cavern availability is an important condition for the stronger hydrogen-side configuration observed in the reference case.

However, heat recovery still retains a positive value even without caverns. The no-caverns scenario remains 0.9 B€/yr cheaper than its paired scenario without heat recovery, and the reduction in DH heat pump capacity remains substantial in the paired comparison. Heat recovery still lowers the capacity of battery. However, the no_caverns scenario has both higher electricity transmission capacity and hydrogen transmission capacity than the no_caverns_no_hr scenario.

4. Discussion

The main results indicate that the value of waste heat recovery is realized through system reallocation across heat, electricity, and hydrogen infrastructures. For the right interpretation of the results of this study, the following limitations are particularly important: the role of district heating network cost, the boundary conditions and the reliance on cost-optimal solutions.

4.1. DH network cost and implications

The cost of the district heating (DH) distribution network is not represented explicitly in this study, although DH demand is imposed

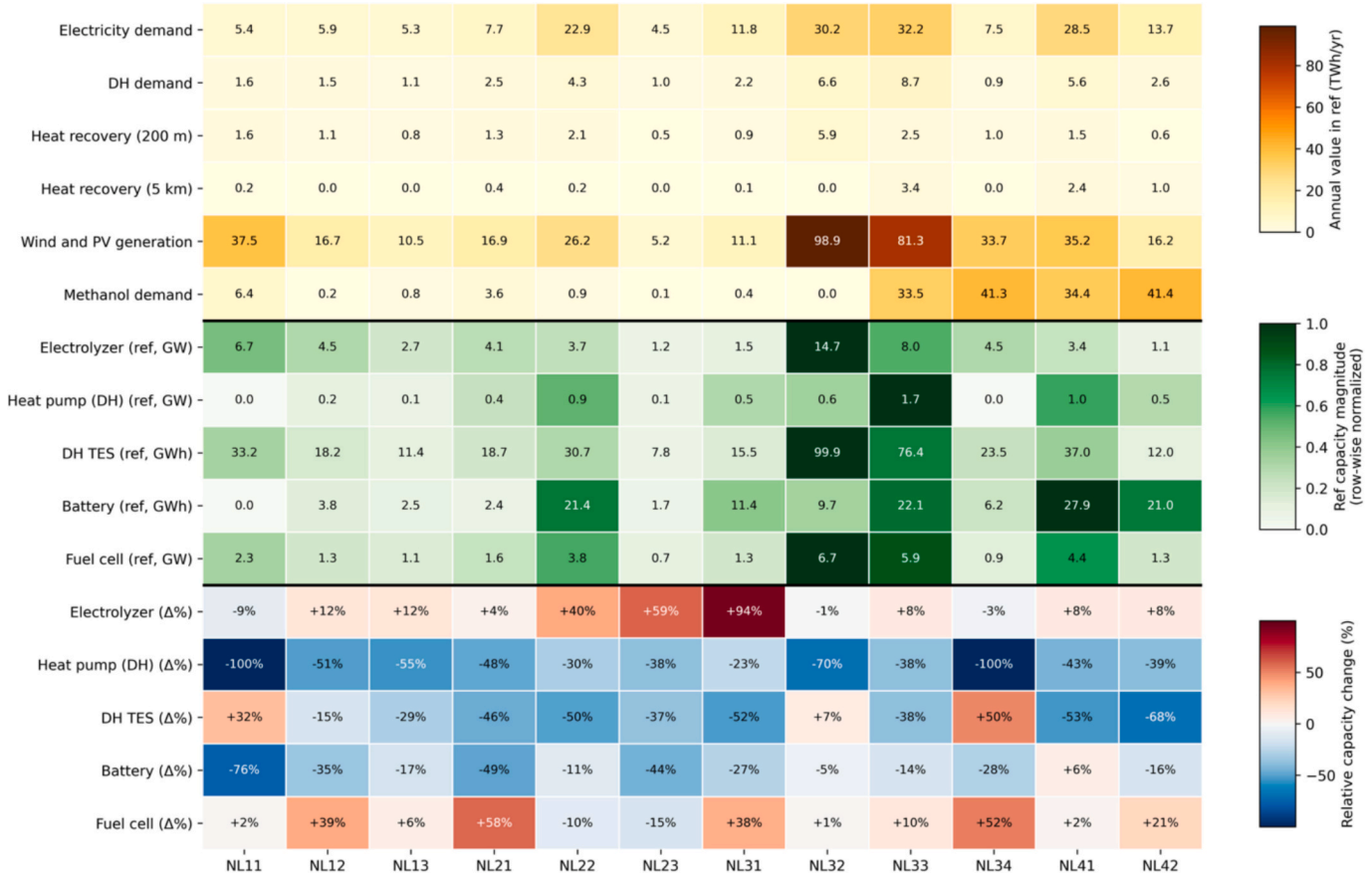

Fig. 5. Provincial demand, recovered heat, and technology reallocation under heat recovery.

exogenously. Under the current demand specification, total heat demand is 96.4 TWh/yr, so the 40% DH-share assumption implies 38.6 TWh/yr of heat delivered through DH. Using the Danish Energy Agency (DEA) "District Heating Distribution, City" benchmark as a starting point, and adjusting it to reflect the higher heat-density conditions that characterize the Dutch urban demand segments identified by Persson et al., the associated DH network investment is estimated at approximately 9.5–10.3 B€, corresponding to an annualized capital cost of about 0.72–0.79 B€/yr under the model discount rate of 7.3% and a 45-year lifetime. Detailed calculation of the DH cost can be found in Supplementary material (C). This omitted cost is economically significant relative to the 1.2 B€/yr system-cost reduction attributed here to waste heat utilization. At the same time, because the DH share is fixed identically across scenarios with and without heat recovery, including DH network cost would mainly shift the absolute system-cost level upward rather than remove the relative advantage of waste heat recovery. The present results should therefore be interpreted as showing the value of recoverable heat conditional on the assumed existence of the DH system, rather than as demonstrating that the DH-based configuration is fully cost-optimal once network rollout costs are included. A more complete assessment would require endogenous optimization of DH network expansion.

The DH-share sensitivity shows that a higher DH share increases the amount of recovered heat that can be utilized, but only moderately improves the relative cost advantage of heat recovery. A larger DH system therefore mainly acts as a higher sink for recoverable heat rather than delivering proportionally higher system savings. This means that higher DH penetration should not automatically be seen as preferable. Since DH expansion also raises network investment costs, its economic attractiveness depends on whether the additional value of utilizing more recovered heat is sufficient to offset the cost of expanding the DH system. This also means that DH deployment and waste heat utilization should be assessed jointly rather than separately.

4.2. *Boundary choices and limitations*

Several boundary choices of the present analysis should be noted:

- The model treats the Netherlands as an electricity self-balancing system without cross-border electricity trade. This assumption is mainly used to make the internal system response to waste-heat recovery easier to interpret. By contrast, methanol imports are allowed, since methanol demand is represented as an annual sink and therefore only needs to be balanced on a yearly basis, whereas electricity demand is modeled hourly and would directly affect short-term balancing and flexibility requirements.
- Biomass is represented in a stylized way through an annual availability bound, without explicit biomass trade representation or intra-annual supply constraints.
- The model does not include all energy-service demands, such as international maritime and aviation fuels.
- Hydrogen boilers for individual and DH heating are not included in the model.
- The model does not include an explicit interprovincial CO_2 transport network and associated cost. This means that CO_2 required for methanol or synthetic methane production must be supplied locally, which may constrain the spatial allocation of DAC and its associated electricity load. However, this effect is likely limited: the supplementary results show that 73% of biomass is used in conversion processes without CO_2 capture, while 75% of CO_2 supply comes from DAC. Therefore, the omission mainly affects DAC siting rather than

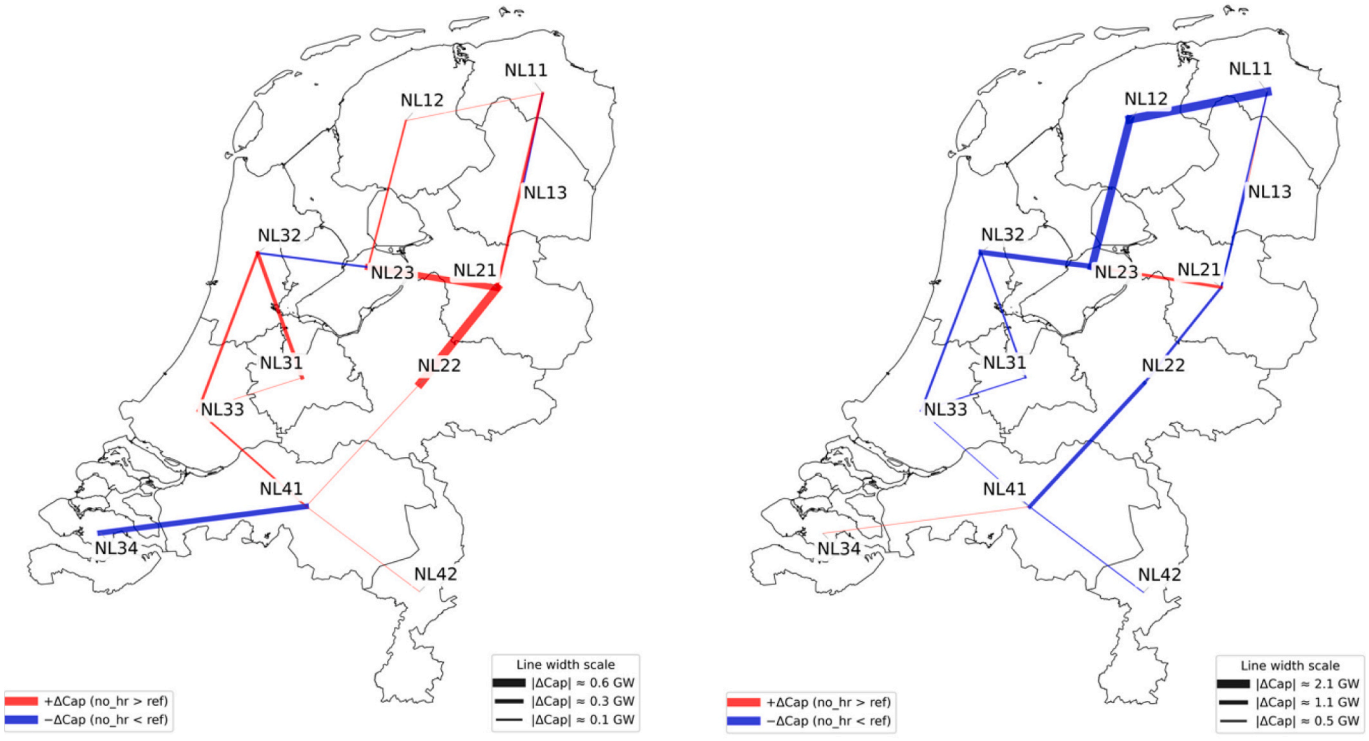

Fig. 6. Spatial difference in newly built network capacities between the no_hr and ref scenarios in 2050 (ΔCap = no_hr − ref). (a) New electricity transmission capacity. (b) New hydrogen pipeline capacity.

Table 10
Summary of key system-level indicators for the reference case and sensitivity scenarios.

Scenario	Sys. cost (B€/yr))	HR benefit (B€/yr)	HR used (TWh/yr)	DH HP (GW)	Battery (GWh)	H_2 cavern (TWh)	Electrolyzer (GW)	New elec. Trans. (GW)	H2 pipe trans. (GW)
ref	59.5		27	9	130	37	45	12	119
no_hr	60.6	1.2	0.0	17	152	33	41	14	108
dh0_6	58.2		32	17	126	36	46	12	118
dh0_6-no_hr	59.4	1.2	0.0	26	146	33	41	14	108
dh0_5	58.8		30	13	128	37	45	12	119
dh0_5-no_hr	60.0	1.2	0.0	21	149	33	41	14	108
dh0_3	58.0		29	11	123	38	46	11	121
dh0_3-no_hr	59.2	1.2	0.0	20	147	34	42	13	110
heat_distance_short	59.4		28	9	130	37	45	12	119
heat_distance_long	59.6		27	9	133	36	44	13	117
heat_distance_10km	59.7		26	9	135	36	44	13	117
dh0_6-10 km	58.5		31	17	133	36	44	14	114
no_caverns	69.6		25	10	203	0	37	12	33
no_caverns_no_hr	70.5	0.9	0.0	16	233.5	0	33.9	11	32

biomass-related technologies and is unlikely to change the main conclusions of this study.

This study reports the average system cost of around 125 €/MWh, calculated as total annualized system cost divided by total energy demand. This is conditional on the system boundary assuming a self-balancing Dutch system without cross-border electricity trade, little conventional firm generation capacity, and a strong reliance on storage.

Several methodological limitations should be acknowledged:

- The model relies on a single weather year and therefore does not capture interannual weather variability, which may affect the estimated role of storage, conversion, and flexibility options because critical periods can differ across years [46].
- The individual effects of the boundary choices listed above are not separately identified here, although they may affect the absolute scale and relative competitiveness of some supply and conversion options.
- This study relies on cost-optimal solutions, with each scenario represented by a single least-cost configuration. This is appropriate for identifying the direction of system design, but it does not imply that all detailed outputs are equally robust. The most reliable conclusions are therefore the system-level ones: waste-heat recovery lowers cost, reduces reliance on electrified DH supply, and reduces dependence on battery-based electricity balancing. By contrast, more detailed spatial siting and transmission network expansion should be interpreted more cautiously, especially under near-optimal alternatives.

Future work could therefore test the robustness of these spatial patterns using near-optimal or alternative-optima analysis.

5. Conclusion

This paper developed a spatially explicit sector-coupled optimization model to assess the system value of heat recovery from electrolyzers, fuel cells, and downstream P2X processes for district heating. Using the Netherlands in 2050 as a case study, the results show that heat recovery can affect both the cost-optimal technology mix and the spatial allocation of conversion capacity.

Heat recovery reduces total annualized system cost from 60.6 to 59.5 B€/yr, corresponding to a saving of about 1.2 B€/yr (2%). It also reduces the need for large district-heating heat pumps from 17 to 9 GW and battery capacity from about 152 to 130 GWh, while increasing electrolyzer capacity from 41 to 45 GW. These results indicate that heat recovery does not only replace part of dedicated district-heating supply, but also changes the system flexibility portfolio by reducing reliance on battery-based electricity balancing and increasing the role of hydrogen-related conversion and storage.

The spatial results show that heat recovery can influence where conversion technologies are located. Electrolyzer capacity shifts partly toward provinces where recovered heat can be used in district heating, indicating that local heat demand can become an important siting factor alongside renewable resource availability and infrastructure conditions.

Sensitivity analysis confirms that the main findings are robust across different assumptions on district-heating share, heat-recovery distance, and hydrogen-cavern availability. Higher district-heating shares generally increase the use of recovered heat, while longer heat-recovery distances reduce its value. Even without hydrogen cavern storage, heat recovery still provides system benefits.

Overall, the study shows that hydrogen- and P2X-related heat recovery should be considered not only as a local efficiency measure, but also as a factor that can influence technology competition, infrastructure use, and spatial planning in sector-coupled energy systems. Future research should test these findings across multiple weather years, broader system boundaries, explicit district-heating network investment, CO_2 transport, and near-optimal system configurations.

CRediT authorship contribution statement

Longquan Li: Writing – original draft, Software, Methodology, Investigation, Formal analysis, Conceptualization. **Francesco Lombardi:** Writing – review & editing, Methodology, Investigation, Conceptualization. **Machteld van den Broek:** Writing – review & editing, Validation, Supervision, Methodology, Investigation, Conceptualization.

Declaration of competing interest

The authors declare that they have no known competing financial interests or personal relationships that could have appeared to influence the work reported in this paper.

Acknowledgments

The author, Longquan Li, receives the financial support from the scholarship granted by China Scholarship Council (CSC, No.202106370021).

Appendix A. Supplementary data

Supplementary data to this article can be found online at https://doi.org/10.1016/j.apenergy.2026.128139.

Data availability

I have shared the link to the data/code in the manuscript

References

[1] Brown T, Schlachtberger D, Kies A, Schramm S, Greiner M. Synergies of sector coupling and transmission reinforcement in a cost-optimised, highly renewable European energy system. Energy 2018;160:720–39.
[2] Vanholme S, Piana S, Hammi I, Ladwa R, Lezamiz Cortazar J, Bianco E. Sector coupling: a key concept for accelerating the energy transformation. 2022.
[3] Ramsebner J, Haas R, Ajanovic A, Wietschel M. The sector coupling concept: a critical review. Wiley Interdiscip Rev Energy Environ 2021;10:e396.
[4] Abdur Rehman O. Enabling technologies for sector coupling: a review on the role of heat pumps and thermal energy storage. Energies 2021;14(24):8195.
[5] Lund H, Werner S, Wiltshire R, Svendsen S, Thorsen JE, Hvelplund F, et al. 4th generation district heating (4GDH): integrating smart thermal grids into future sustainable energy systems. Energy 2014;68:1–11.
[6] Werner S. International review of district heating and cooling. Energy 2017;137:617–31.
[7] Ramsebner J. The sector coupling concept: a critical review. WIREs Energy Environ 2021.
[8] Action ICf. Sector coupling: a key concept for accelerating the energy transition. International Renewable Energy Agency; 2022.
[9] Van Der Roest E, Bol R, Fens T, van Wijk A. Utilisation of waste heat from PEM electrolysers–unlocking local optimisation. Int J Hydrog Energy 2023;48:27872–91.
[10] Burrin D, Roy S, Roskilly AP, Smallbone A. A combined heat and green hydrogen (CHH) generator integrated with a heat network. Energy Convers Manag 2021;246:114686.
[11] Meriläinen A, Kosonen A, Jokisalo J, Kosonen R, Kauranen P, Ahola J. Techno-economic evaluation of waste heat recovery from an off-grid alkaline water electrolyzer plant and its application in a district heating network in Finland. Energy 2024;306:132181.
[12] Vandenberghe R, Humbert G, Cai H, Koirala BP, Sansavini G, Heer P. Optimal sizing and operation of hydrogen generation sites accounting for waste heat recovery. Appl Energy 2025;380:125004.
[13] Koumparakis C, Kountouris I, Bramstoft R. Utilization of excess heat in future power-to-X energy hubs through sector-coupling. Appl Energy 2025;377:124098.
[14] Tommasini D, Marx N, Wimmer Y, Reuter S, Kauko H. Electrolysis waste heat utilization for district heating—a Norwegian case study. Smart Energy 2025:100207.
[15] Pan G, Gu W, Lu Y, Qiu H, Lu S, Yao S. Optimal planning for electricity-hydrogen integrated energy system considering power to hydrogen and heat and seasonal storage. IEEE Transact Sustain Energy 2020;11:2662–76.
[16] Pfenninger S, Pickering B. Calliope: a multi-scale energy systems modelling framework. J Open Source Softw 2018;3:825.
[17] Shirizadeh B, Quirion P. Do multi-sector energy system optimization models need hourly temporal resolution? A case study with an investment and dispatch model applied to France. Appl Energy 2022;305:117951.
[18] Pickering B, Lombardi F, Pfenninger S. Diversity of options to eliminate fossil fuels and reach carbon neutrality across the entire European energy system. Joule 2022;6:1253–76.
[19] Quintel. Energy transition model dataset manager. 2026.
[20] Quintel. Energy transition model. 2026.
[21] Nederland N. II3050 eindrapport. 2023.
[22] OPSD. Time series. 2026.
[23] Averfalk H, Werner S. Economic benefits of fourth generation district heating. Energy 2020;193:116727.
[24] van der Roest E, Bol T. Utilisation of waste heat from PEM electrolysers: unlocking local optimisation. Int J Hydrog Energy 2023;48(72):27872–91.
[25] Coalition NE. The Dutch hydrogen economy in 2050. 2019.
[26] Tröndle T, Pfenninger S, Lilliestam J. Home-made or imported: on the possibility for renewable electricity autarky on all scales in Europe. Energ Strat Rev 2019;26:100388.
[27] Rijksoverheid. Wind op zee. 2026.
[28] TNO. Technology-Factsheet-wind-onshore. 2021.
[29] Staffell I, Pfenninger S. Using bias-corrected reanalysis to simulate current and future wind power output. Energy 2016;114:1224–39.
[30] Pfenninger S, Staffell I. Long-term patterns of European PV output using 30 years of validated hourly reanalysis and satellite data. Energy 2016;114:1251–65.
[31] Sollai S, Porcu A, Tola V, Ferrara F, Pettinau A. Renewable methanol production from green hydrogen and captured CO2: a techno-economic assessment. J CO_2 Util 2023;68:102345.
[32] DEA. Technology data for generation of electricity and district heating. 2026.
[33] argus. Argus biomass markets weekly biomass markets news and analysis wednesday 9 July 2025. 2025.
[34] Bioenergy I. Implementation of bioenergy in the Netherlands – 2024 update. 2024.
[35] Juez-Larré J, Van Gessel S, Dalman R, Remmelts G, Groenenberg R. Assessment of underground energy storage potential to support the energy transition in the Netherlands. First Break 2019;37:57–66.
[36] Hörsch J, Hofmann F, Schlachtberger D, Brown T. PyPSA-Eur: an open optimisation model of the European transmission system. Energ Strat Rev 2018;22:207–15.

[37] DEA. Technology data for energy storage. 2026.
[38] DEA. Technology data for transport of energy. 2026.
[39] Manz P, Kermeli K, Persson U, Neuwirth M, Fleiter T, Crijns-Graus W. Decarbonizing district heating in EU-27+ UK: how much excess heat is available from industrial sites? Sustainability 2021;13:1439.
[40] DEA. Technology data for renewable fuels. 2026.
[41] Böhm H, Zauner A, Rosenfeld DC, Tichler R. Projecting cost development for future large-scale power-to-gas implementations by scaling effects. Appl Energy 2020; 264:114780.
[42] DEA. Technology data for individual heating plants. 2026.
[43] DEA. Technology data for industrial process heat. 2026.
[44] Markussen WB, Rosenow J, Christensen MH, Zühlsdorf B, Elmegaard B. Techno-economic analysis of technologies for decarbonizing low-and medium-temperature industrial heat. Cell Rep Sustain 2025;2.
[45] DEA. Technology data for carbon capture, transport and storage. 2026.
[46] Hawkins D, Van Den Broek M, Bruninx K. Exploring the impact of interannual dynamics on long-duration energy storage in energy system models. In: 2025 21st international conference on the European energy market. EEM: IEEE; 2025. p. 1–6.